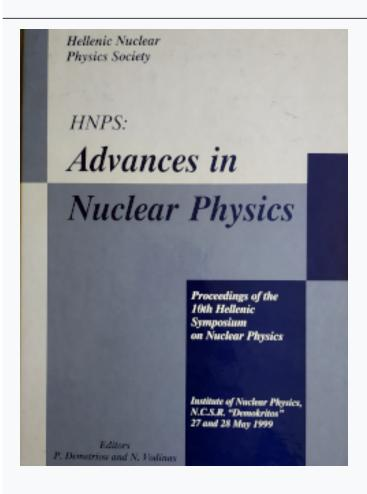




HNPS Advances in Nuclear Physics

Vol 10 (1999)

HNPS1999



The 3-Dimensional g-Deformed Harmonic Oscillator and a Unified Description of Magic Numbers of Metal Clusters

N. Karoussos, Dennis Bonatsos, P. P. Raychev, R. P. Roussev

doi: 10.12681/hnps.2192

To cite this article:

Karoussos, N., Bonatsos, D., Raychev, P. P., & Roussev, R. P. (2019). The 3-Dimensional g-Deformed Harmonic Oscillator and a Unified Description of Magic Numbers of Metal Clusters. *HNPS Advances in Nuclear Physics*, *10*, 215–230. https://doi.org/10.12681/hnps.2192

The 3-Dimensional q-Deformed Harmonic Oscillator and a Unified Description of Magic Numbers of Metal Clusters

N. Karoussos^a, Dennis Bonatsos^a, P. P. Raychev^b and R. P. Roussev^b

- ^a Institute of Nuclear Physics, NCSR "Demokritos", GR-153 10 Aghia Paraskevi, Athens, Greece
 - b Institute for Nuclear Research and Nuclear Energy, Bulgarian Academy of Sciences, 72 Tzarigrad Road, BG-1784 Sofia, Bulgaria

Abstract

Magic numbers predicted by a 3-dimensional q-deformed harmonic oscillator with $\mathbf{u}_q(3) \supset \mathbf{so}_q(3)$ symmetry are compared to experimental data for atomic clusters of alkali metals (Li, Na, K, Rb, Cs), noble metals (Cu, Ag, Au), divalent metals (Zn, Cd), and trivalent metals (Al, In), as well as to theoretical predictions of jellium models, Woods–Saxon and wine bottle potentials, and to the classification scheme using the 3n+l pseudo quantum number. In alkali metal clusters and noble metal clusters the 3-dimensional q-deformed harmonic oscillator correctly predicts all experimentally observed magic numbers up to 1500 (which is the expected limit of validity for theories based on the filling of electronic shells), while in addition it gives satisfactory results for the magic numbers of clusters of divalent metals and trivalent metals, thus indicating that $\mathbf{u}_q(3)$, which is a nonlinear extension of the $\mathbf{u}(3)$ symmetry of the spherical (3-dimensional isotropic) harmonic oscillator, is a good candidate for being the symmetry of systems of several metal clusters.

1 Introduction

Metal clusters have been recently the subject of many investigations (see [1-4] for relevant reviews). One of the first fascinating findings in their study was the appearance of magic numbers, analogous to but different from the magic numbers appearing in the shell structure of atomic nuclei [5]. Different kinds of metallic clusters [alkali metals (Na [6-9], Li [10,11], K [12], Rb [13], Cs [7,14,15]), noble metals (Cu [16,17], Ag [16,18], Au [16]), divalent metals of the IIB group (Zn, Cd) [19], trivalent metals of the III group (Al, In) [20]] exhibit different sets of magic

numbers. The analogy between the magic numbers observed in metal clusters and the magic numbers observed in atomic nuclei led to the early description of metal clusters in terms of the Nilsson—Clemenger model [21], which is a simplified version of the Nilsson model [22,23] of atomic nuclei, in which no spin-orbit interaction is included. Further theoretical investigations in terms of the jellium model [24,25] demonstrated that the mean field potential in the case of simple metal clusters bears great similarities to the Woods—Saxon potential of atomic nuclei, with a slight modification of the "wine bottle" type [26]. The Woods—Saxon potential itself looks like a harmonic oscillator truncated at a certain energy value and flattened at the bottom. It should also be recalled that an early schematic explanation of the magic numbers of metallic clusters has been given in terms of a scheme intermediate between the level scheme of the 3-dimensional harmonic oscillator and the square well [1]. Again in this case the intermediate potential resembles a harmonic oscillator flattened at the bottom.

On the other hand, modified versions of harmonic oscillators [27,28] have been recently investigated in the novel mathematical framework of quantum algebras [29,30], which are nonlinear generalizations of the usual Lie algebras. The spectra of q-deformed oscillators increase either less rapidly (for q being a phase factor, i.e. $q = e^{i\tau}$ with τ being real) or more rapidly (for q being real, i.e. $q = e^{\tau}$ with τ being real) in comparison to the equidistant spectrum of the usual harmonic oscillator [31], while the corresponding (WKB-equivalent) potentials [32] resemble the harmonic oscillator potential, truncated at a certain energy (for q being a phase factor) or not (for q being real), the deformation inflicting an overall widening or narrowing of the potential, depending on the value of the deformation parameter q.

Very recently, a q-deformed version of the 3-dimensional harmonic oscillator has been constructed [33], taking advantage of the $\mathbf{u}_q(3) \supset \mathbf{so}_q(3)$ symmetry [34,35]. The spectrum of this 3-dimensional q-deformed harmonic oscillator has been found [33] to reproduce very well the spectrum of the modified harmonic oscillator introduced by Nilsson [22,23], without the spin-orbit interaction term. Since the Nilsson model without the spin orbit term is essentially the Nilsson-Clemenger model used for the description of metallic clusters [21], it is worth examining if the 3-dimensional q-deformed harmonic oscillator can reproduce the magic numbers of simple metallic clusters. This is the subject of the present investigation.

In Section 2 the 3-dimensional q-deformed harmonic oscillator will be briefly described, while in Section 3 the magic numbers provided by this oscillator will be compared with the experimental data for Na and Li clusters, as well as with the predictions of other theories (jellium model, Woods–Saxon and wine bottle potentials, classification scheme using the 3n+l pseudo quantum number). Additional comparisons of magic numbers predicted by the 3-dimensional q-deformed harmonic oscillator to experimental data and to the results of other theoretical approaches will be made in Section 4 (for other alkali metal clusters and noble metal clusters), Section 5 (for divalent group IIB metal clusters), and Section 6 (for trivalent group III metal clusters), while Section 7 will contain discussion of the present results and plans for further work.

2 The 3-dimensional q-deformed harmonic oscillator

The space of the 3-dimensional q-deformed harmonic oscillator consists of the completely symmetric irreducible representations of the quantum algebra $\mathbf{u}_q(3)$. In this space a deformed angular momentum algebra, $\mathbf{so}_q(3)$, can be defined [33]. The Hamiltonian of the 3-dimensional q-deformed harmonic oscillator is defined so that it satisfies the following requirements:

- a) It is an $so_q(3)$ scalar, i.e. the energy is simultaneously measurable with the q-deformed angular momentum related to the algebra $so_q(3)$ and its z-projection.
- b) It conserves the number of bosons, in terms of which the quantum algebras $u_q(3)$ and $so_q(3)$ are realized.
- c) In the limit $q \to 1$ it is in agreement with the Hamiltonian of the usual 3-dimensional harmonic oscillator.

It has been proved [33] that the Hamiltonian of the 3-dimensional q-deformed harmonic oscillator satisfying the above requirements takes the form

$$H_q = \hbar\omega_0 \left\{ [N]q^{N+1} - \frac{q(q-q^{-1})}{[2]} C_q^{(2)} \right\},\tag{1}$$

where N is the number operator and $C_q^{(2)}$ is the second order Casimir operator of the algebra $so_q(3)$, while

$$[x] = \frac{q^x - q^{-x}}{q - q^{-1}} \tag{2}$$

is the definition of q-numbers and q-operators.

The energy eigenvalues of the 3-dimensional q-deformed harmonic oscillator are then [33]

$$E_q(n,l) = \hbar\omega_0 \left\{ [n]q^{n+1} - \frac{q(q-q^{-1})}{[2]}[l][l+1] \right\},\tag{3}$$

where n is the number of vibrational quanta and l is the eigenvalue of the angular momentum, obtaining the values l = n, n - 2, ..., 0 or 1.

In the limit of $q \to 1$ one obtains $\lim_{q \to 1} E_q(n, l) = \hbar \omega_0 n$, which coincides with the classical result. For small values of the deformation parameter τ (where $q = e^{\tau}$) one can expand Eq. (3) in powers of τ obtaining [33]

$$E_{\sigma}(n,l) = \hbar\omega_0 n - \hbar\omega_0 \tau \left(l(l+1) - n(n+1)\right)$$

$$-\hbar\omega_0\tau^2\left(l(l+1) - \frac{1}{3}n(n+1)(2n+1)\right) + \mathcal{O}(\tau^3). \tag{4}$$

Eq. (4) to leading order bears great similarity to the modified harmonic oscillator suggested by Nilsson [22,23] (with the spin-orbit term omitted)

$$V = \frac{1}{2}\hbar\omega\rho^2 - \hbar\omega\kappa'(\mathbf{L}^2 - \langle \mathbf{L}^2 \rangle_N), \qquad \rho = r\sqrt{\frac{M\omega}{\hbar}}, \tag{5}$$

where

$$<\mathbf{L}^2>_N=\frac{N(N+3)}{2}.$$
 (6)

The energy eigenvalues of Nilsson's modified harmonic oscillator are [22,23]

$$E_{nl} = \hbar\omega n - \hbar\omega\mu' \left(l(l+1) - \frac{1}{2}n(n+3) \right). \tag{7}$$

It has been proved [33] that the spectrum of the 3-dimensional q-deformed harmonic oscillator closely reproduces the spectrum of the modified harmonic oscillator of Nilsson. In both cases the effect of the l(l+1) term is to flatten the bottom of the harmonic oscillator potential, thus making it to resemble the Woods–Saxon potential.

The level scheme of the 3-dimensional q-deformed harmonic oscillator (for $\hbar\omega_0=1$ and $\tau=0.038$) is given in Table 1, up to a certain energy. Each level is characterized by the quantum numbers n (number of vibrational quanta) and l (angular momentum). Next to each level its energy, the number of particles it can accommodate (which is equal to 2(2l+1)) and the total number of particles up to and including this level are given. If the energy difference between two successive levels is larger than 0.39, it is considered as a gap separating two successive shells and the energy difference is reported between the two levels. In this way magic numbers can be easily read in the table: they are the numbers appearing above the gaps, written in boldface characters.

Calculating additional level schemes of the 3-dimensional q-deformed harmonic oscillator (for different values of the parameter τ) we remark that the small magic numbers do not change much as the parameter τ is varied, while large magic numbers get more influenced by the parameter modification.

3 Sodium and lithium clusters

The magic numbers provided by the 3-dimensional q-deformed harmonic oscillator in Table 1 are compared to available experimental data for Na clusters [6-9] and Li

Table 1 Energy spectrum, $E_q(n,l)$, of the 3-dimensional q-deformed harmonic oscillator (Eq. (3)), for $\hbar\omega_0=1$ and $q=e^{\tau}$ with $\tau=0.038$. Each level is characterized by n (the number of vibrational quanta) and l (the angular momentum). 2(2l+1) represents the number of particles each level can accommodate, while under "total" the total number of particles up to and including this level is given. Magic numbers, reported in boldface, correspond to energy gaps larger than 0.39, reported between the relevant couples of energy levels.

\overline{n}	l	$E_q(n,l)$	2(2l+1)	total	n	l	$E_q(n,l)$	2(2l+1)	total
0	0	0.000	2	2			0.502		
		1.000			7	5	8.396	22	220
1	1	1.000	6	8	8	8	8.494	34	254
		1.006					0.627		
2	2	2.006	10	18	7	3	9.121	14	268
2	0	2.243	2	20			0.397		
		0.780			7	1	9.518	6	274
3	3	3.023	14	34	9	9	9.709	38	312
		0.397			8	6	9.743	26	338
3	1	3.420	6	40			0.894		
		0.638			8	4	10.637	18	356
4	4	4.058	18	58	10	10	10.980	42	398
		0.559			9	7	11.146	30	428
4	2	4.617	10	68	8	2	11.196	10	438
4	0	4.854	2	70	8	0	11.434	2	440
5	5	5.116	22	92			0.781		
		0.724			9	5	12.215	22	462
5	3	5.841	14	106	11	11	12.315	46	508
6	6	6.204	26	132	10	8	12.614	34	542
5	1	6.238	6	138	9	3	12.939	14	556
		0.860					0.397		
6	4	7.098	18	156	9	1	13.336	6	562
7	7	7.328	30	186	12	12	13.721	50	612
6	2	7.657	10	196	10	6	13.863	26	638
6	0	7.895	2	198	11	9	14.154	38	676

clusters [10,11] in Table 2 (columns 2-7). The following comments apply:

- i) Only magic numbers up to 1500 can be considered, since it is known that filling of electronic shells is expected to occur only up to this limit [6]. For large clusters beyond this point it is known that magic numbers can be explained by the completion of icosahedral or cuboctahedral shells of atoms [6].
- ii) Up to 600 particles there is consistency among the various experiments and between the experimental results in one hand and our findings in the other.
- iii) Beyond 600 particles the results of the four experiments, which report magic numbers in this region, are quite different. However, the results of all four experiments are well accommodated by the present model. In addition, each magic number predicted by the model is supported by at least one experiment. This holds not only up to the magic number 1012, included in Table 2, but up to the magic number 1500, not shown in Table 2 because of space limitations.

In Table 2 the predictions of a simple theoretical model [5], the rounded square well potential which is intermediate between the non-deformed 3-dimensional harmonic oscillator and the square well potential, are also reported (in column 8) for comparison. It is clear that the predictions of this model are in partial agreement with the experimental data up to the magic number 138, since the model fails by predicting magic numbers at 68, 70, 106, 112, 156, which are not observed.

It should be noticed at this point that the first few magic numbers of alkali clusters (up to 92) can be correctly reproduced by the assumption of the formation of shells of atoms instead of shells of delocalized electrons [36], this assumption being applicable under conditions not favoring delocalization of the valence electrons of alkali atoms.

Comparisons among the present results, experimental data for Na clusters (by Martin et al. [6] (column 2) and Pedersen et al. [9] (column 3)), experimental data for Li clusters (Bréchignac et al. [10] (column 4)), and theoretical predictions more sophisticated than these reported in Table 2, can be made in Table 3, where magic numbers predicted by various jellium model calculations (columns 5 and 6, [2,37]), Woods–Saxon and wine bottle potentials (column 7, [38]), as well as by a classification scheme using the 3n+l pseudo quantum number (column 8, [6]) are reported. The following observations can be made:

- i) All magic numbers predicted by the 3-dimensional q-deformed harmonic oscillator are supported by at least one experiment, with no exception.
- ii) The jellium models, as well as the 3n+l classification scheme, predict magic numbers at 186, 540/542, which are not supported by experiment. The jellium models also predict a magic number at 748 or 758, again without support from experiment. The Woods-Saxon and wine bottle potentials of Ref. [38] predict a magic number at 68, for which no experimental support exists. The present scheme avoids problems at these numbers. It should be noticed, however, that in the cases of 186 and 542 the energy gap following them in the present scheme is 0.329 and

Table 2 Magic numbers provided by the 3-dimensional q-deformed harmonic oscillator (Table 1), reported in column 1, are compared to the experimental data for Na clusters by Martin et al. [6] (column 2), Bjørnholm et al. [7] (column 3), Knight et al. [8] (column 4), and Pedersen et al. [9] (column 5), as well as to the experimental data for Li clusters by Bréchignac et al. ([10] in column 6, [11] in column 7). The magic numbers provided [5] by a rounded square well potential intermediate between the (non-deformed) 3-dimensional harmonic oscillator and the square well potential are also shown (in column 8) for comparison. See text for discussion.

th.	exp.	exp.	exp.	exp.	exp.	exp.	th.
present	Na	Na	Na	Na	Li	Li	int.
Tab. 1	Ref.[6]	Ref.[7]	Ref.[8]	Ref.[9]	Ref.[10]	Ref.[11]	Ref.[5]
2	2	2	2			2	2
8	8	8	8			8	8
(18)	18						18
20	20	20	20			20	20
34	34						34
40	40	40	40	40		40	40
58	58	58	58	58		58	58
							68,70
92	90,92	92	92	92	93	92	92
							106,112
138	138	138		138	134	138	138
198	$198{\pm}2$	196		198	191	198	156
254		260 ± 4				258	
268	$263{\pm}5$			264	262		
338	341 ± 5	344 ± 4		344	342	336	
440	443 ± 5	440 ± 2		442	442	440	
556	557 ± 5	558 ± 8		554	552	546	
676				680			
694	$700{\pm}15$				695	710	
832	$840 {\pm} 15$			800	822	820	
912					902		
1012	1040±20			970	1025	1065	
							Company Compan

Table 3 Magic numbers provided by the 3-dimensional q-deformed harmonic oscillator (Table 1), reported in column 1, are compared to the experimental data for Na clusters by Martin $et\ al.\ [6]\ (column\ 2)$, and Pedersen $et\ al.\ [9]\ (column\ 3)$, as well as to the experimental data for Li clusters by Bréchignac $et\ al.\ [10]\ (column\ 4)$ and to the theoretical predictions of various jellium model calculations reported by Brack [2] (column\ 5) and Bulgac and Lewenkopf [37] (column\ 6), the theoretical predictions of Woods–Saxon and wine bottle potentials reported by Nishioka $et\ al.\ [38]\ (column\ 7)$, as well as to the magic numbers predicted by the classification scheme using the 3n+l pseudo quantum number, reported by Martin $et\ al.\ [6]\ (column\ 8)$. See text for discussion.

th.	exp.	exp.	exp.	th.	th.	th.	th.
present	Na	Na	Li	jell.	jell.	WS	3n + l
Tab. 1	Ref.[6]	Ref.[9]	Ref.[10]	Ref.[2]	Ref.[37]	Ref.[38]	Ref.[6]
2	2			2		2	2
8	8			8		8	8
(18)	18						18
20	20			20		20	
34	34			34	34		34
40	40	40				40	
58	58	58		58	58	58	58
						68	
92	90,92	92	93	92	92	92	90
138	138	138	134	138	138	138	132
				186	186		186
198	198 ± 2	198	191			198	
254				254	254	254	252
268	263 ± 5	264	262			268	
338	341 ± 5	344	342	338	338	338	332
440	443 ± 5	442	442	438,440	440	440	428
				542	542		540
556	557 ± 5	554	552	556	556	562	
676		680		676	676		670
694	700 ± 15		695			694	
				758	748		

0.325 respectively (see Table 1), i.e. quite close to the threshold of 0.39 which we have considered as the minimum energy gap separating different shells. One could therefore qualitatively remark that 186 and 542 are "built in" the present scheme as "secondary" (not very pronounced) magic numbers.

4 Other alkali metals and noble metals

Experimental data for various additional alkali metal clusters [K [12], column 2), Rb ([13], column 3), Cs [7,14], column 4)] and for various noble metal clusters [Cu ([16], column 5), Ag [18] in column 6 and [16] in column 7), Au ([16], column 8)] are reported in Table 4, along with the theoretical predictions of the 3-dimensional q-deformed harmonic oscillator given in Table 1. The following comments apply:

- i) In the cases of Rb [13], Cu [16], Ag [16], Au [16], what is seen experimentally is cations of the type Rb_N^+ , Cu_N^+ , Ag_N^+ , Au_N^+ , which contain N atoms each, but N-1 electrons. The magic numbers reported in Table 6 are electron magic numbers in all cases.
- ii) All alkali metals and noble metals shown in Tables 2 and 4 give the same magic numbers, at least within the ranges reported in the tables. For most of these metals the range of experimentally determined magic numbers is rather limited, with Na [6], Cs [7,14], Li [10], and Ag [18] being notable exceptions.
- iii) The magic numbers occurring in Na [6], Cs [7,14], Li [10], and Ag [18] are almost identical, and are described very well by the oscillator of Table 1. The limited data on K, Rb, Cu, Au, also agree with the magic numbers of Table 1.

5 Divalent metals of the IIB group

For these metals the quantities determined experimentaly [19] are numbers of atoms exhibiting "magic" behaviour. Each atom has two valence electrons, therefore the magic numbers of electrons are twice the magic numbers of atoms. The magic numbers of electrons for Zn and Cd clusters [19] are reported in Table 5 (in columns 4 and 5 respectively), along with the magic numbers predicted by the 3-dimensional q-deformed harmonic oscillator for two different parameter values (reported in columns 1 and 2 respectively), and the magic numbers given by a potential intermediate between the simple harmonic oscillator and the square well potential ([19], column 3). The following comments can be made:

- i) The experimental magic numbers for Zn and Cd [19] are almost identical. Magic numbers reported in parentheses are "secondary" magic numbers, while the magic numbers without parentheses are the "main" ones, as indicated in [1].
- ii) In column 1 of Table 5 magic numbers of the 3-dimensional q-deformed harmonic

Table 4
Magic numbers provided by the 3-dimensional q-deformed harmonic oscillator (Table 1), reported in column 1, are compared to the experimental data for clusters of K [12] (column 2), Rb [13] (column 3), Cs [7,14] (column 4), Cu [16] (column 5), Ag ([18] in column 6, [16] in column 7), and Au [16] (column 8). See text for discussion.

th.	exp.	exp.	exp.	exp.	exp.	exp.	exp.
present	K	Rb	Cs	Cu	Ag	Ag	Au
Tab.1	Ref.[12]	Ref.[13]	Ref.[7,14]	Ref.[16]	Ref.[18]	Ref.[16]	Ref.[16]
2	2	2	2	2		2	2
8	8	8	8	8	8	8	8
(18)		18	18				
20	20	20	20	20	20	20	20
34		34	34	34	34	34	34
40	40	40	40	40	(40)	40	
58	58		58	58	58	58	58
92			92	92	92	92	92
138			138	138	138	138	138
198			198 ± 2		186 ± 4	198	
254							
268			263 ± 5		$268{\pm}5$		
338			341 ± 5		338 ± 15		
440			$443{\pm}5$		440 ± 15		
556			557 ± 5				
676							
694			700 ± 15				
832			840 ± 15				
912							
1012			1040 ± 15				

oscillator with $\tau=0.038$ and energy gaps larger than 0.26 are reported. Decreasing the energy gap considered as separating different shells from 0.39 (used in Table 1) to 0.26 (used in Table 5) has as a result that the numbers 70 and 106 become magic, in close agreement with the experimental data. Similar but even better results are gotten from the 3-dimensional q-deformed harmonic oscillator reported in column 2 of Table 5. This oscillator is characterized by $\tau=0.020$, while the energy gap

Table 5 Magic numbers provided by the 3-dimensional q-deformed harmonic oscillator of Table 1 with energy gap equal to 0.26 (column 1) and by a 3-dimensional q-deformed harmonic oscillator characterized by $\tau=0.020$ and energy gap equal to 0.20 (column 2), are compared to the experimental data for Zn clusters [19] (column 4) and Cd clusters [19] (column 5), as well as to the theoretical predictions of a potential intermediate between the simple harmonic oscillator and the square well potential [19] (column 3). In addition, the magic numbers provided by a 3-dimensional q-deformed harmonic oscillator charactrized by $\tau=0.050$ and energy gap equal to 0.38 (reported in column 6) are compared to the experimental data for Al [20] (column 7) and In [20] (column 8). See text for discussion.

th. th. th. exp. exp. th. exp. present Present Al In $\tau=0.038$ $\tau=0.02$ Ref.[19] Ref.[19] Ref.[19] r=0.05 Ref.[20] Ref.[20] 2 2 2 138 138 138 8 8 164 164 164 20 20 20 20 186 164 188 34 34 34 (36) (36) 198 198 40 40 40 40 254 252 252 58 58 56 56 338 336 336 70 70 70 70 486 468±6 468±6 80 (64) (64) 440 438 468±6 468±6 92 92 92 92 676 688±6 468±6 106 106 102 108 108 748 <t< th=""><th></th><th></th><th></th><th></th><th></th><th></th><th></th><th></th></t<>								
$\begin{array}{c ccccccccccccccccccccccccccccccccccc$	th.	th.	th.	exp.	exp.	th.	exp.	exp.
$\begin{array}{cccccccccccccccccccccccccccccccccccc$	present	present		$\mathbf{Z}\mathbf{n}$	Cd	present	Al	In
$\begin{array}{cccccccccccccccccccccccccccccccccccc$	τ =0.038	τ =0.02	Ref.[19]	Ref.[19]	Ref.[19]	$\tau = 0.05$	Ref.[20]	Ref.[20]
$\begin{array}{c ccccccccccccccccccccccccccccccccccc$	2	2				138	138	138
$\begin{array}{c ccccccccccccccccccccccccccccccccccc$	8	8					164	
$\begin{array}{c ccccccccccccccccccccccccccccccccccc$	20	20	20	20	20	186		
$\begin{array}{c ccccccccccccccccccccccccccccccccccc$	34	34	34	(36)	(36)		198	198
$\begin{array}{c ccccccccccccccccccccccccccccccccccc$	40	40	40	40	40	254		252
$\begin{array}{c ccccccccccccccccccccccccccccccccccc$	58	58	58	56	56	338	336	
$\begin{array}{c ccccccccccccccccccccccccccccccccccc$				(60)	(60)	398		
$ \begin{array}{c ccccccccccccccccccccccccccccccccccc$			68	(64)	(64)	440	438	
$\begin{array}{c ccccccccccccccccccccccccccccccccccc$	70	70	70	70	70	486	468 ± 6	
$\begin{array}{cccccccccccccccccccccccccccccccccccc$				(80)	(80)	542	534 ± 6	
$\begin{array}{c ccccccccccccccccccccccccccccccccccc$				(82)		612	594 ± 6	
$\begin{array}{c ccccccccccccccccccccccccccccccccccc$	92	92	92	92	92	676	688 ± 6	
$ \begin{array}{c ccccccccccccccccccccccccccccccccccc$	106	106	102	108	108	748	$742{\pm}6$	
$\begin{array}{c ccccccccccccccccccccccccccccccccccc$		112	112	(114)		832	832 ± 10	
1006 1000±10 1074 1100 1112±10				(120)	(120)	890		
1074 1100 1112±10	138	138	138	138	138	912	$918{\pm}10$	
1100 1112±10						1006	1000 ± 10	
						1074		
1206 1224±10						1100	1112±10	
						1206	1224±10	

between different shells is set equal to 0.20 . We observe that the second oscillator predicts an additional magic number at 112, in agreement with experiment, but otherwise gives the same results as the first one. We remark therefore that the general agreement between the results given by the 3-dimensional q-deformed harmonic oscillator and the experimental data is not sensitively dependent on the parameter value, but, in contrast, quite different parameter values ($\tau=0.038,\,\tau=0.020$) provide quite similar sets of magic numbers (at least in the region of relatively small magic numbers).

iii) Both oscillators reproduce all the "main" magic numbers of Zn and Cd, while the intermediate potential between the simple harmonic oscillator and the square well potential, reported in column 3, reproduces all the "main" magic numbers except 108.

6 Trivalent metals of the III group

Magic numbers of electrons for the trivalent metals Al and In [20] are reported in Table 5 (in columns 7 and 8 respectively), along with the predictions of a 3-dimensional q-deformed harmonic oscillator with $\tau=0.050$ and energy gap separating different shells equal to 0.38 (column 6). The following comments can be made:

- i) It is known [1,20] that small magic numbers in clusters of Al and In cannot be explained by models based on the filling of electronic shells, because of symmetry breaking caused by the ionic lattice [20], while for large magic numbers this problem does not exist.
- ii) The magic numbers predicted by the 3-dimensional q-deformed harmonic oscillator reported in column 6 of Table 5 agree quite well with the experimental findings, with an exception in the region of small magic numbers, where the model fails to reproduce the magic numbers 164 and 198, predicting only a magic number at 186. In addition the oscillator predicts magic numbers at 398, 890, 1074, which are not seen in the experiment reported in column 7.

7 Discussion

The following general remarks can now be made:

i) From the results reported above it is quite clear that the 3-dimensional q-deformed harmonic oscillator describes very well the magic numbers of alkali metal clusters and noble metal clusters in all regions, using only one free parameter ($q = e^{\tau}$ with $\tau = 0.038$). It also provides an accurate description of the "main" magic numbers of clusters of divalent group IIB metals, either with the same parameter value ($\tau = 0.038$) or with a different one ($\tau = 0.020$). In addition it gives a satisfactory

description of the magic numbers of clusters of trivalent group III metals with a different parameter value ($\tau = 0.050$).

- ii) It is quite remarkable that the 3-dimensional q-deformed harmonic oscillator reproduces long sequences of magic numbers (Na, Cs, Li, Ag) at least as accurately as other, more sophisticated, models by using only one free parameter ($q = e^{\tau}$). Once the parameter is fixed, the whole spectrum is fixed and no further manipulations can be made. This can be considered as evidence that the 3-dimensional q-deformed harmonic oscillator owns a symmetry (the $u_q(3) \supset so_q(3)$ symmetry) appropriate for the description of the physical systems under study.
- iii) It has been remarked [6] that if n is the number of nodes in the solution of the radial Schrödinger equation and l is the angular momentum quantum number, then the degeneracy of energy levels of the hydrogen atom characterized by the same n+l is due to the $\mathrm{so}(4)$ symmetry of this system, while the degeneracy of energy levels of the spherical harmonic oscillator (i.e. of the 3-dimensional isotropic harmonic oscillator) characterized by the same 2n+l is due to the $\mathrm{su}(3)$ symmetry of this system. 3n+l has been used [6] to approximate the magic numbers of alkali metal clusters with some success, but no relevant Lie symmetry could be determined (see also [39.40]). In view of the present findings the lack of Lie symmetry related to 3n+l is quite clear: the symmetry of the system appears to be a quantum algebraic symmetry $(\mathrm{u}_q(3))$, which is a nonlinear extension of the Lie symmetry $\mathrm{u}(3)$.
- iv) An interesting problem is to determine a WKB-equivalent potential giving (within this approximation) the same spectrum as the 3-dimensional q-deformed harmonic oscillator, using methods similar to these of Ref. [32]. The similarity between the results of the present model and these provided by the Woods–Saxon potential (column 7 in Table 3) suggests that the answer should be a harmonic oscillator potential flattened at the bottom, similar to the Woods–Saxon potential. If such a WKB-equivalent potential will show any similarity to a wine bottle shape, as several potentials used for the description of metal clusters do [24–26], remains to be seen.

In summary, we have shown that the 3-dimensional q-deformed harmonic oscillator with $\mathbf{u}_q(3) \supset \mathbf{so}_q(3)$ symmetry correctly predicts all experimentally observed magic numbers of alkali metal clusters and of noble metal clusters up to 1500, which is the expected limit of validity for theories based on the filling of electronic shells. In addition it gives a good description of the "main" magic numbers of group IIB (divalent) metal clusters, as well as a satisfactory description of group III (trivalent) metal clusters. This indicates that $\mathbf{u}_q(3)$, which is a nonlinear deformation of the $\mathbf{u}(3)$ symmetry of the spherical (3-dimensional isotropic) harmonic oscillator, is a good candidate for being the symmetry of systems of several metal clusters.

Acknowledgements

One of the authors (PPR) acknowledges support from the Bulgarian Ministry of Science and Education under contract Φ -547, while another author (NK) has been supported by the Greek General Secretariat of Research and Technology under

References

- [1] W. A. de Heer, Rev. Mod. Phys. 65 (1993) 611.
- [2] M. Brack, Rev. Mod. Phys. 65 (1993) 677.
- [3] V. O. Nesterenko, Fiz. Elem. Chastits At. Yadra 23 (1992) 1665 [Sov. J. Part. Nucl. 23 (1992) 726.
- [4] W. A. de Heer, W. D. Knight, M. Y. Chou and M. L. Cohen, Solid State Phys. 40 (1987) 93.
- [5] M. G. Mayer and J. H. D. Jensen, Elementary Theory of Nuclear Shell Structure (Wiley, New York, 1955).
- [6] T. P. Martin, T. Bergmann, H. Göhlich and T. lange, Chem. Phys. Lett. 172 (1990) 209; Z. Phys. D 19 (1991) 25.
- [7] S. Bjørnholm, J. Borggreen, O. Echt, K. Hansen, J. Pedersen and H. D. Rasmussen, Phys. Rev. Lett. 65 (1990) 1627; Z. Phys. D 19 (1991) 47.
- [8] W. D. Knight, K. Clemenger, W. A. de Heer, W. A. Saunders, M. Y. Chou and M. L. Cohen, Phys. Rev. Lett. 52 (1984) 2141.
- [9] J. Pedersen, S. Bjørnholm, J. Borggreen, K. Hansen, T. P. Martin and H. D. Rasmussen, Nature 353 (1991) 733.
- [10] C. Bréchignac, Ph. Cahuzac, M. de Frutos, J.-Ph. Roux and K. Bowen, in Physics and Chemistry of Finite Systems: From Clusters to Crystals, edited by P. Jena et al. (Kluwer, Dordrecht, 1992), Vol. 1, p. 369.
- [11] C. Bréchignac, Ph. Cahuzac, F. Carlier, M. de Frutos and J. Ph. Roux, Phys. Rev. B 47 (1993) 2271.
- [12] W. D. Knight, W. A. de Heer, K. Clemenger and W. A. Saunders, Solid State Commun. 53 (1985) 445.
- [13] N. D. Bhaskar, R. P. Frueholz, C. M. Klimcak and R. A. Cook, Phys. Rev. B 36 (1987) 4418.
- [14] H. Göhlich, T. Lange, T. Bergmann and T. P. Martin, Phys. Rev. Lett. 65 (1990) 748.
- [15] T. Bergmann, H. Limberger and T. P. Martin, Phys. Rev. Lett. 60 (1988) 1767.
- [16] I. Katakuse, T. Ichihara, Y. Fujita, T. Matsuo, T. Sakurai and H. Matsuda, Int. J. Mass Spectrom. Ion Processes 67 (1985) 229.
- [17] M. B. Knickelbein, Chem. Phys. Lett. 192 (1992) 129.

- [18] G. Alameddin, J. Hunter, D. Cameron and M. M. Kappes, Chem. Phys. Lett. 192 (1992) 122.
- [19] I. Katakuse, T. Ichihara, Y. Fujita, T. Matsuo, T. Sakurai and H. Matsuda, Int. J. Mass Spectrom. Ion Processes 69 (1986) 109.
- [20] J. L. Persson, R. L. Whetten, H. P. Cheng and R. S. Berry, Chem. Phys. Lett. 186 (1991) 215.
- [21] K. Clemenger, Phys. Rev. B 32 (1985) 1359.
- [22] S. G. Nilsson, Mat. Fys. Medd. Dan Vid. Selsk. 29, no 16 (1955).
- [23] S. G. Nilsson and I. Ragnarsson, *Shapes and Shells in Nuclear Structure* (Cambridge University Press, Cambridge, 1995).
- [24] W. Ekardt, Ber. Bunsenges. Phys. Chem. 88 (1984) 289; Phys. Rev. B 29 (1984) 1558.
- [25] D. E. Beck, Solid State Commun. 49 (1984) 381; Phys. Rev. B 30 (1984) 6935.
- [26] B. A. Kotsos and M. E. Grypeos, in Atomic and Nuclear Clusters, edited by G. S. Anagnostatos and W. von Oertzen (Springer, Berlin, 1995), p. 242.
- [27] L. C. Biedenharn, J. Phys. A 22 (1989) L873.
- [28] A. J. Macfarlane, J. Phys. A 22 (1989) 4581.
- [29] V. Chari and A. Pressley, A Guide to Quantum Groups (Cambridge University Press, Cambridge, 1994).
- [30] A. Klimyk and K. Schmüdgen, Quantum Groups and Their Representations (Springer, Berlin, 1997).
- [31] D. Bonatsos, C. Daskaloyannis, P. Kolokotronis and D. Lenis, Rom. J. Phys. 41 (1996) 109.
- [32] D. Bonatsos, C. Daskaloyannis and K. Kokkotas, J. Math. Phys. 33 (1992) 2958.
- [33] P. P. Raychev, R. P. Roussev, N. Lo Iudice and P. A. Terziev, J. Phys. G 24 (1998) 1931.
- [34] Yu. F. Smirnov, V. N. Tolstoy and Yu. I. Kharitonov, Yad. Fiz. 54 (1991) 721 [Sov. J. Nucl. Phys. 54 (1991) 437];
 - Yu. F. Smirnov and Yu. I. Kharitonov, Yad. Fiz. 56 (1993) 263;

Phys. At. Nucl. 56 (1993) 1143;

Yad. Fiz. 59 (1996) 379;

Phys. At. Nucl. 59 (1996) 360;

A. A. Malashin, Yu. F. Smirnov and Yu. I. Kharitonov, Yad. Fiz. 58 (1995) 651;

Phys. At. Nucl. 58 (1995) 595;

Yad. Fiz. 58 (1995) 1105;

Phys. At. Nucl. 58 (1995) 1031.

[35] J. Van der Jeugt, J. Phys. A 25 (1992) L213; J. Math. Phys. 34 (1993) 1799; Can. J. Phys. 72 (1994) 519.

- [36] G. S. Anagnostatos, Phys. Lett. A 154 (1991) 169.
- [37] A. Bulgac and C. Lewenkopf, Phys. Rev. Lett. 71 (1993) 4130.
- [38] H. Nishioka, K. Hansen and B. R. Mottelson, Phys. Rev. B 42 (1990) 9377.
- [39] E. Koch, Phys. Rev. A 54 (1996) 670.
- [40] V. N. Ostrovsky, Phys. Rev. A 56 (1997) 626.